Corrales Ureña et al. Applied Adhesion Science (2015) 3:7
DOI 10.1186/s40563-015-0032-6

Applied Adhesion Science
a SpringerOpen Journal

RESEARCH Open Access

Influences of the pH on the adsorption properties of an antimicrobial peptide on titanium surfaces

Yendry Regina Corrales Ureña[1,2*], Linda Wittig[2], Matheus Vieira Nascimento[2,3], Juliano Luiz Faccioni[2,4], Paulo Noronha Lisboa Filho[5] and Klaus Rischka[2]

* Correspondence: yendry386@hotmail.com
[1]Programa de Pós-Graduação em Ciência e Tecnologia de Materiais (POSMAT), São Paulo State University (UNESP), Av. Eng. Luiz Edmundo Carrijo Coube 14-01, 17033-360, Bauru, São Paulo, Brazil
[2]Fraunhofer Institute for Manufacturing Technology and Advanced Materials (IFAM), Wiener Straße 12, 28359 Bremen, Germany
Full list of author information is available at the end of the article

Abstract

The adsorption behavior of the Tet-124 antimicrobial peptide and the Tet-124 peptide modified at the C- and N-terminus with the sequence glycine-3,4-dihydroxyphenylalanine-glycine (G-DOPA-G) on titanium surfaces was studied using quartz crystal micro balance with dissipation (QCM-D). At a low pH level (4.75) Tet-124 and Tet-124-G-DOPA-G form rigid layers. This is attributed to the electrostatic interactions of the positively charged lysine and arginine residues in the peptide sequence with the negatively charged titanium oxide layer. At an elevated pH level (6.9) Tet-124 shows a lower mass adsorption at the surface than Tet-124-G-DOPA-G. This is attributed to the interaction of the catechol due to the formation of complexes with the titanium oxide and titanium surface layer. The C terminal and N terminal modification with the sequence G-DOPA-G shows similar adsorption rate and mass adsorption coverage at saturation; however it is presented a more loosely layers on the G-DOPA-G-TeT-124. Fibroblast adhesion and the biocompatibility test of both the surfaces following modification with Tet-124-G-DOPA-G and the titanium alloy control showed similar results. In addition, no changes in the adhesion of *E. coli* bacteria due to the modification of the surface were detected.

Keywords: Titanium; Implants; Peptide; DOPA; Adsorption; Antimicrobial

Background

Ti-alloys have been the subject of a number of studies and are commonly used as implant material due to their good biocompatibility, mechanical properties and corrosion resistance [1]. However infections caused by contamination on the implant surface can lead to serious problems [2]. Different surface modification strategies have been studied to prevent infections associated with bacteria settlement with the aim of enabling the long term resiliencece [1,3] of the implant [4]. The use of antimicrobial peptides [5], nanostructured noble metal coatings [6], composites coatings [7] as hydroxyapatite/titanium [8] and polysaccharide-based coatings consisting of chitosan and alginate [9] have so far been studied.

Antimicrobial peptides have recently been investigated for their broad antimicrobial activity against gram-positive and gram-negative bacteria [10] as well as for their immunomodulatory properties [11]. Antimicrobial peptides are produced by the immune systems of all multicellular organisms in nature [12]. Being part of the innate defenses

of animals, insects and plants [13], they have been studied as an alternative to classic antibiotics for overcoming problems such as multidrug resistance [4].

Antimicrobial peptides typically consist of 12 to 100 amino acids [14] and are amphiphilic molecules with a high content of cationic and hydrophobic amino acids [12] that are responsible for the antibacterial activity [14]. In general the mechanisms of action against bacteria are attributed to the interaction and disruption of the bacterial membranes [15].

Strategies for antimicrobial peptide immobilization on surfaces generally exploit monovalent or covalent reactions [16]. Hilpert *et al*. studied peptides covalently bonded to cellulose membranes [13] showing bacterial growth inhibition. Furthermore Haynie et *al*. demonstrated promising results of antimicrobial peptides covalently bonded to a polyamide resin using solid-phase peptide synthesis [17].

The antimicrobial peptide sequence used for immobilization in this research was based on a peptide previously synthesized by Hilpert *et al*., the Tet-124 sequence KLWWMIRRW, which shows a minimum inhibitory concentration (MIC) of 8 μg/ml against *Pseudomonas aeruginosa* strain H1001. They tested 122 sequences, however not all peptides with higher levels of bacterial growth inhibition in solution showed the same inhibition when tethered to the membrane.

The immobilization strategy is based on the electrostatic interactions of the peptide with a titanium alloy surface (Ti-6Al-4 V; alloy composition: approximately 6% aluminum, 4% vanadium and 90% titanium) and the modification of both N- and C- terminus with G-DOPA-G, changing the original sequence to KLWWMIRRW-G-DOPA-G (Tet-124-G-DOPA-G) and G-DOPA-GKLWWMIRRW (G-DOPA-G-Tet-124). The DOPA amino acid was added to the sequences to promote adhesion to titanium alloy surfaces by the catechol moiety due the possible formation complexes with the metal and metal oxide surface [18]. Richter *et al.* studied the surface coverage and adsorption rate by QCM of different decapeptide sequences derived from the cuticle mussel protein (mefp1) with different lengths and different DOPA content [19] on titanium surfaces. An increase in the DOPA content was correlated to a higher adsorption on the titanium substrates.

The main objective of this research is to immobilize an antimicrobial peptide on a titanium surface and to study the impact of the surface modifications related to bacterial and cell adhesion.

Methods

Solid-phase peptide synthesis

The peptides Tet-124, G-DOPA-G-Tet-124 and Tet-124-G-DOPA-G were synthesized in a 433A solid-phase peptide synthesizer (Applied Biosystems, Farmington, CT, USA) using the FastMoc™-protocol. DOPA was introduced into the sequences as (2S)-3-(2,2-dimethyl-1,3-benzodioxol-5-yl)-2-(9H-fluoren-9-ylmethoxycarbonylamino)propanoic acid (Fmoc-DOPA (acetonoid)-OH) during the syntheses. The syntheses were carried out in a 0.1 mmol scale using either Fmoc-glycine or Fmoc-tryptophan (Boc) preloaded tritylchloride resin (TCP). The amino acids were obtained from IRIS Biotech, Marktredwitz, Germany and Fmoc-DOPA (acetonoid)-OH from Merck-NovaBiochem, Hohenbrunn, Germany. TCP resins were purchased from Intavis AG, Heidelberg, Germany with a loading of approx. 0.55 mmol/g.

The cleavage and the removal of the side chain protecting groups of the peptide from the resin was performed with a solution consisting of 3600 μL trifluoroacetic acid, 200 μL deionized water and 200 μL triisopropylsilane. After the synthesis the resins were treated with the cleavage solution for two hours. The peptides were obtained through precipitation of the cleavage solutions in 60 ml ice cold *tert.*-butyl methyl ether after filtration through a syringe filter (polytetrafluoroethylene membrane, diameter 13 mm, pore width 0.45 μm). After centrifugation the precipitates were separated from the ether solution and dissolved in deionized water; the peptides were obtained after lyophilization as a colorless powder.

The characterization of the peptides was undertaken by using a BioCad 700E high precision liquid chromatography system (HPLC) (Applied Biosystems). A Varian HPLC column was used to analyze the samples (Polaris 5u C18-A, 250 × 46 mm). In addition, the peptides were characterized on a time-of-flight mass spectrometer (MALDI-ToF-MS) Voyager DE-Pro manufactured by Applied Biosystems, Foster City, USA (matrix: α-cyano-4-hydroxycinnamic acid (CHCA) from Sigma-Aldrich, Steinheim, Germany); the purity of the obtained peptides was 95% or higher. All the peptides were stored at −20°C.

Sample preparation

Commercial available titanium-aluminum-vanadium-alloy (Ti-6Al-4 V) substrates were used. The surfaces were emeried before being submerged in 0.3 mg/ml Tet-124-G-DOPA-G in sodium acetate buffer solution 0.1 M (pH = 4.75). The samples were rinsed with deionized ater and the liquid film was blown away from surface using pressurized air; the samples were dried under environmental conditions.

Contact angle Measurements

The apparent contact angles were measured using a goniometer (OCA15 Plus, Data Physics Instruments, Germany) by sessile drop technique and HPLC grade water (Across Organics) was used as liquid probe. The volume of the drops was kept constant (10 μL) for each measurement. The contact angle values represent an an average value of at least three separate drops on different substrate areas. The recorded images were analyzed by SCAN 20 Data Physics software.

QCM-D

Quartz crystal micro balance with dissipation (QCM-D, Q-Sense E4, Sweden) was used to evaluate the adsorption on titanium QCM-D sensors (QSX 310, Q-Sense, Sweden). The sensors are gold-coated quartz crystals with a diameter of 14 mm with a 50 nm thick Ti layer. Titanium and TiO_2 anatase are the main phases detected on these titanium coated QCM-D crystals [20].

The adsorption due to the crystal contact with the peptide solution was monitored in real time for all the overtones (n = 1, 3, 5, 7…) at a temperature of 25°C. Before use, the crystal stayed in the UV/ozone chamber for 15 min to remove contaminants from the surface. The sensors were mounted in the flow module and the system was equilibrated for 10 min to constant temperature. Next the flow cells were filled with a buffer and the buffer was pumped through the cells at a slow and constant flow of 100 μL/min. The sensors were equilibrated with the buffer solution until similar frequencies and

dissipation values (D) were achieved for all the different overtones. The buffer flow was kept constant for 30 min to ensure that the baseline was stable and then the system was stopped for maximum of 1 min and the buffer container was exchanged with the peptide solution containers, after which the solutions were pumped into the system. The experiments were carried out in a flow-cell set-up with a constant flow rate of 100 μL/min. Changes in the resonance frequency, f, related to attached mass (including coupled water), and in the dissipation (D), related to frictional (viscous) losses in the adlayer, were recorded using QSoftTM control software (supplied by the QCM-D instrument). The buffer used was sodium acetate buffer 0.1 M, solution pH 4.75 (measurement results figure 2, 3) and deionized water with a conductivity of <50 μS (measurements results figure 4, 5, 6). The frequency and dissipation was analyzed by applying the Sauerbrey model with the QToolsTM software (supplied with the QCM-D instrument).

The adsorbed mass was calculated using the Sauerbrey equation (1). The Sauerbrey theory is based on the assumption that mass loading attached to the quartz crystal shows ideal acoustic coupling to the crystal surface and that the crystal is an infinite plane [20]. The Sauerbrey equation is used when mass deposition forms a thin (approximately the mass loading of up to 0.05% of the crystal mass) and rigid layer, which is determined by the changes of the dissipation coefficient [21]:

$$\Delta f = -\frac{f_R}{\rho_Q dA}\Delta m = -\frac{f_R}{nA}\Delta m = -\frac{C\Delta m}{n} \tag{1}$$

Where Δm is the mass gain at the electrode surface (in ng /cm^2), f_R is the fundamental resonance frequency of the quartz crystal, ρ_Q is the density of the crystal, d is the thickness of the quartz crystal (~330 nm), A is the area of the electrodes and n is the overtone number used in the determination (n = 1, 3, 5. . .13). The relation of resonance frequency divided by the electrode area is known as the mass sensitivity constant (C) value (17.7 ng Hz^{-1} cm^{-2}). The mass sensitive is assumed to be uniform over the entire surface in this experiment and no smoothing of the experimental data it is applied for calculations.

The dissipation coefficient was detected in parallel. Dissipation occurs when the driving voltage to the crystal is shut off and the energy from the oscillating crystal dissipates from the system; the resonant frequency of the quartz crystal (f_0) is mixed with f_R and filtered with a low pass band filter. This gives an output frequency (f) based on the difference between f_R and f_0. This difference frequency is fitted to an exponentially damped sinusoidal (equation 2). The frequency penetration depth (in the z direction away from the sensor surface) depends on the material in question and typically is on the order of 250 nm.

$$A(t) = A_0\ e^{\frac{t}{\tau}} sin(2\pi f t + \alpha) \tag{2}$$

Where τ is the decay time constant,

A(t) is the oscillation amplitude, t is the time, A_0 is the amplitude at t = 0. D is defined as the relation between the energy lost during one oscillation cycle (E_{lost}) and the total energy stored in the oscillator (E_{stored}) as shown in equation 3 [22]:

$$D = \frac{1}{\pi f \tau} = \frac{E_{lost}}{2\pi E_{stored}} \tag{3}$$

This procedure can be repeated over 200 times per second, which gives QCM-D a great level of sensitivity and high resolution [23].

Cell Culture

L929 Cells were cultured in 75 cm^2 cell culture flasks (CellStar, Sigma-Aldrich) under 37°C, 5% CO_2 and humidified atmosphere; the culture medium was prepared mixing Roswell Park Memorial Institute (RPMI) 1640 medium with L-Glutamine (Lonza), 10% of fetal bovine serum (Biochrom AG), penicillin (100 μg/mL), and 100 μg/mL streptomycin (Lonza) under aseptic conditions (biological safety cabinet, Thermo Scientific). First the medium was removed from the culture flask by an air pump (Vacuubrand BVC 21NT) using a Pasteur pipette. Cells were washed with 4 mL phosphate buffered saline (PBS buffer, concentration 0.01 M, Sigma-Aldrich, Germany) prior to adding 1 mL of a Trypsin solution 1% in PBS (Lonza, Germany). Following this the flask was brought to the incubator (Sanyo MCO-18AIC) for 10 min and the cell concentration in the liquid was determined by passing an aliquot from the culture flask and to a 96-well plate. 15 μL from this aliquote was mixed with 15 μL trypan blue. Trypan blue is a dye unable to penetrate healthy cells, so they remain unstained. Dead cells have a compromised cell membrane that is permeable to the trypan blue dye. Dead cells are stained blue and display as dark cells that can be identified by the Cellometer software with bright field imaging.

20 μL of the resulting solution was pipetted in the counting chamber of the cell counter (Cellometer Auto T4 from Nexcelom Bioscience) and the cell concentration was obtained. During cell counting procedures, the culture flask was taken placed in ashaker (IKA KS260, Basic) at 100 rpm, in order to avoid cell reattachment. Finally, a volume corresponding to a quantity of 1×10^6 cells was pipetted into a new culture flask, and culture media was added to a final volume of 20 mL. The assay was performed using samples approximately 50% of the area modified with Tet-124-G-DOPA-G and the other 50% of the area not modified which served as control (half modified sample). Prior to cell seeding, samples were sterilized under UV light for at least 15 min. 1 mL of cell solution in fresh medium was added on each sample at a seeding density of 1×10^5 cells/mL. Samples were taken to the incubator for 24 h. After the incubation period the medium was removed and samples were washed two times with 1 mL PBS buffer. After each wash, but before removal of the washing solution, samples were briefly shaken at 100 rpm. Fixation was performed by adding 1 mL of 2.5% glutaraldehyde in PBS on the samples and leaving them in the fridge overnight. Following fixation, samples were washed again twice with PBS and stained with Alexa Fluor 568 Phalloidin and NucBlue Live ReadyProbes (both from Life Technologies), according to the manufacturer's instructions [24]. Alexa Fluor stains the actin filaments of the cytoskeleton with a red fluorescent color, while NucBlue stains the nuclei blue. After each staining protocol, samples were washed with twice with PBS. Results were observed by fluorescence microscopy (Zeiss) at the wavelengths recommended by the manufacturers [24].

Bacteria adhesion

The attachment of *Escherichia coli* (*E.coli*, DSM 10290) on 1 cm^2 Ti-6Al-4 V substrates modified with Tet-124-G-DOPA-G and unmodified (control) was evaluated. *E. coli*

colonies obtained from an agar plate were incubated at 37°C in 5 ml of Luria Bertani (LB) broth medium for 16 h (overnight culture). The overnight culture was centrifuged and the supernatant was removed. The remaining pellet was suspended in minimal medium (MM, 1 ml of LB mixed with 99 ml of PBS). This step was repeated three times. The concentration of the bacterial solution (approx.1×10^6 colony-forming units/ml (CFU/ml)) was adjusted by measuring the optical density (O.D.) at 600 nm (with an absorbance of 0.06 corresponding to 2×10^8 CFU/ml). 50 μL of the bacterial solution was pipetted onto the substrates, followed by the placement of a coverslip (10×10 mm) and an incubation time of 4 h at 37°C. Subsequently, the samples were rinsed three times by pipetting up and down 150 μL of PBS. The samples underwent a bacterial detachment procedure based on the ISO 22196; they were put into 50 mL centrifuge tubes which were subsequently filled with PBS until the substrate was totally immersed. The tubes were transported to an ultrasonic cleaner (Sonorex RK100 Bandelin Electronic, Berlin, Germany) where they remained for 3 min and thereafter agitated in a vortex mixer (IKA–Werke GmbH & Co. KG, Staufen, Germany) for 1 min. To investigate the presence of bacteria in the solutions, 200 μL of the first rinse water and 200 μL of the 50 mL centrifuge tubes, respectively, were transferred to a 96-well microplate and 50 μL of LB was additionally pipetted in each well. The PBS and the LB used for the experiments were also analyzed to make sure they were sterile. The variation in the optical density of these solutions (absorbance at 620 nm) against time was measured at 37°C for 24 h with a microplate multimode reader (Mithras LB 940, Berthold Technologies, Germany). The samples were stained with the LIVE/DEAD® BacLight Bacterial Viability Kit (Invitrogen, Molecular Probes) and were examined with a fluorescence microscope (Zeiss Axio Imager M1, Carl Zeiss, Jena, Germany).

Results and discussions

The C- and the N-terminus of the Tet-124 peptide was modified with the sequence G-DOPA-G to study the adsorption behavior due to the potential interaction of the catechol moieties [19] with the oxide titanium layer. The DOPA amino acid was flanked by two glycine amino acids to avoid an intramolecular crosslinking with the neighbored amino groups, both of the N-terminus and of the lysine. For a better comparison regarding chain length and molecular mass Tet-124-G-DOPA-G was flanked by glycine as well.

Figure 1 shows the amino acid sequence of the peptide Tet-124 and the modifications due the addition on the C- and N-terminal with the G-DOPA-G sequence.

Figure 2A shows the adsorption behavior of the titanium coated sensors in contact with the Tet-124-G-DOPA-G peptide in sodium acetate buffer. During the first five minutes of the experiment the crystal is flushed by the pure buffer remaining in the system (i.e. tubings, module). The change to the peptide solution results in a constant frequency. Following this the peptide solution comes into contact with the crystal surface. There is a decrease in the crystal resonance frequency indicating mass adsorption. During this period the first four minutes show a higher adsorption rate. After approximately 15 minutes the surface has become saturated; presenting an equilibrium between adsorption and desorption. The D coefficient shows small changes during the significant changes in frequency, as can be seen in Figure 2B. The dissipation values

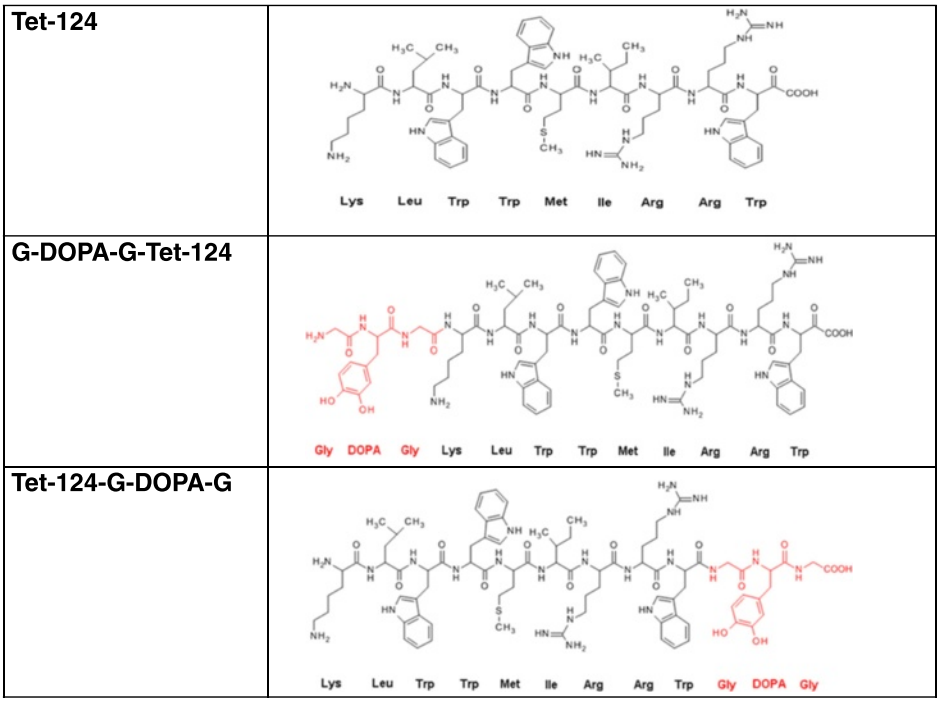

Figure 1 Scheme sequence Tet-124, G- DOPA-G-Tet-124 and Tet-124-G-DOPA-G.

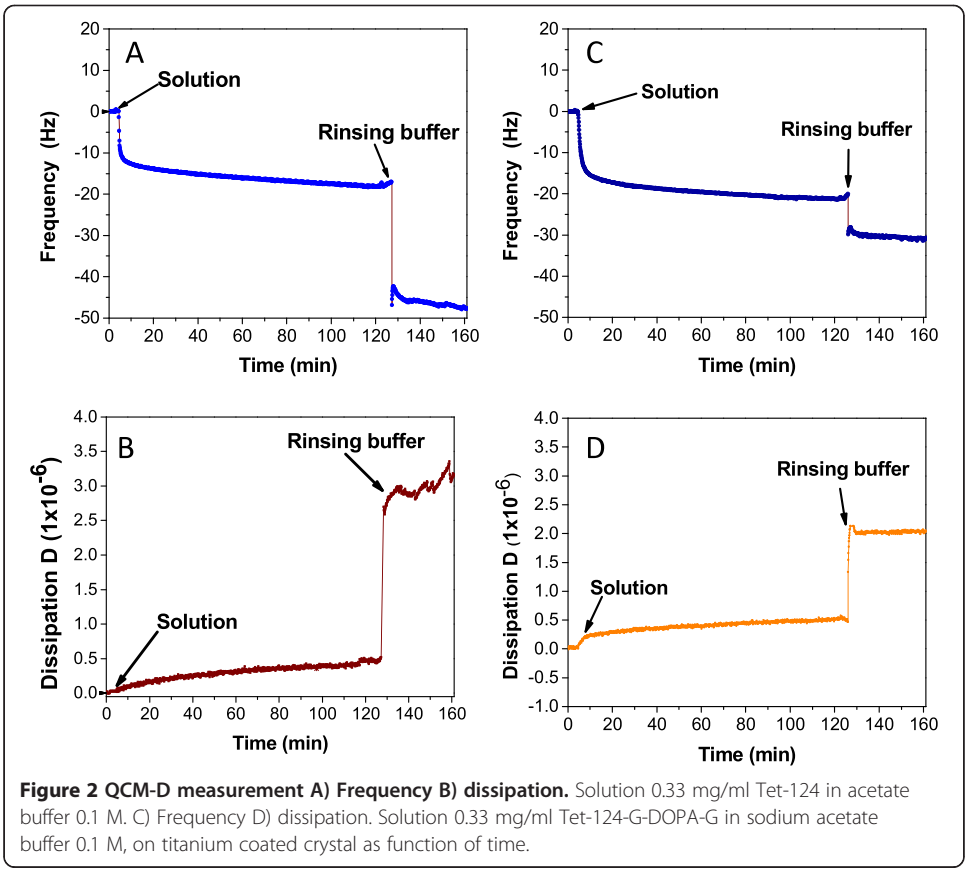

Figure 2 QCM-D measurement A) Frequency B) dissipation. Solution 0.33 mg/ml Tet-124 in acetate buffer 0.1 M. C) Frequency D) dissipation. Solution 0.33 mg/ml Tet-124-G-DOPA-G in sodium acetate buffer 0.1 M, on titanium coated crystal as function of time.

depends on the amplitude decaying over time, which is related to such a parameters as the oscillator, the contact medium, size and kind of molecule, temperature etc. In general typical values for frequency decreases due to mass adsorption of proteins are between 10–100 Hz and dissipation coefficient values of tens $\times 10^{-6}$ units [22]. For rigid films the typically changes on the dissipation coefficient are in the order of $1\text{-}10\times 10^{-6}$ [25]. A small value means that the adlayer has less deformation and/or internal friction with the surface. High D values are mostly obtained due to a high damping of the oscillating crystal that is normally originated from soft layers which don´t follow the sensor oscillation, producing internal friction caused by deformation; also could be related to loosely bonded molecules [22,26]. Additionally, the dissipation coefficient depends on the interactions of the molecule with water. If the molecules attached to the surface adsorb high quantities of water, the resulting surface is highly dissipative [22]. However low dissipation coefficients do not necessarily mean "strong bonded molecules" [23]. The antimicrobial peptide is consisted of 50% hydrophobic amino acids and possesses a low solubility in water (0.5 mg/ml maximum, 25°C). For this reason the rising step with buffer solution is fundamental to determine the stability (no desorption) of the film in the surface.

After two hours the surface was rinsed with buffer solution for 30 min and no desorption at the surface was detected. After changing from peptide to buffer solution the dissipation and the spread of the overtones increased drastically. This is typically associated with solvent uptake, leading to a swelling of the film coming along with a film property change from rigid to soft [27].

Due the small changes on the dissipation coefficient the Sauerbrey equation was used for the calculation of the adsorbed mass. Figure 3A shows a saturation value of approx. 316 ng/cm^2. During the measurement only one step was detected (rapid decrease of the frequency follow by a stabilization) that could be related to a formation of a monolayer.

A broad calculation related to the occupied molecule area was performed. The area occupied by a dopamine molecule on a gold surface is 0.194 nm^2 accordingly to Sebok *et al.* [28]. The adsorbed quantity of Tet-124-G-DOPA-G (molecular weight 1612 g/mol) is 1.4 μg/cm^2, assuming the occupied area of a DOPA moiety is similar to that of dopamine on gold. It is expected the value may be smaller due to such factors like the random adsorption, not well-ordered pattern across the whole area and

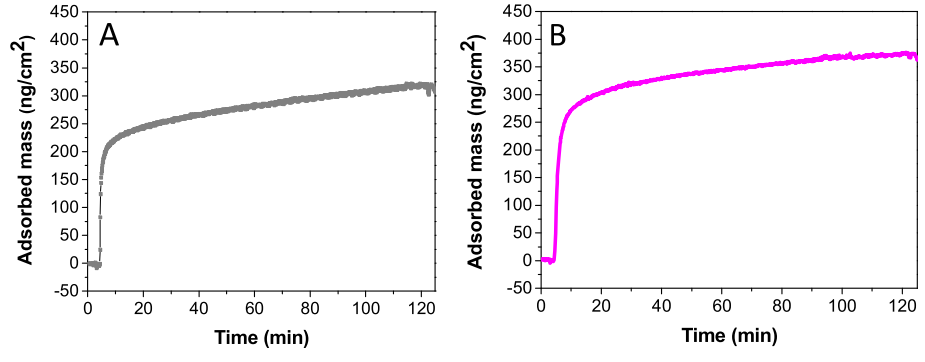

Figure 3 Mass changes obtained from peptide solution on titanium coated sensor, 0.33 mg/ml in acetate buffer 0.1 M A) Tet-124 B)Tet-124-G-DOPA-G.

the adsorbed water molecules [25]. A typical protein layer has values of 500 – 1000 ng/cm^2 [25]. The theoretical isoelectric points (pI) of the synthesized peptides were calculated using the Protein calculator v3.4 [28]. The pI value of the peptides G-DOPA-G-Tet-124 and Tet-124-G-DOPA-G is approximately 11.5. For this reason at a pH of 4.75 it is expected that the amino acids lysine and arginine will be positively charged and it could be repulsion between the positively charged peptides molecules.A monolayer formation is suggested.

Using the QCM-D software parameters such as layer thickness, viscosity or shear forces can be calculated to a certain degree when is a clear spreading of the frequency values for the different overtones and D is higher than 1 $\times 10^{-6}$. The obtained results show lower D values and no clear spreading of the overtones frequency values (data not shown). The layer thickness was estimated to 2.86 nm with an intermediate density value of 1.1 kg/m^3 between a protein film 1.3 kg/m^3 and a water film with density of 1 kg/m^3 [29].

Figure 2C shows similar adsorption rate behavior of Tet-124 when compared with Tet-124-G-DOPA-G. No significant differences on the adsorption rate were detected. The surface coverage after saturation was 365 ng/cm^2; layer thickness 3.31 nm. According to the low changes in the dissipation coefficient a rigid layer was formed and multilayer formation was not detected for two hours. Similar adsorption rates between the two peptides may be expected due to their similar molecular length [30].

The isoelectric point of the titanium coated quartz crystal sensors was measured by Cuddy *et al.* [31], showing that the isoelectric point is approximately 2.9. In general solid oxides in aqueous suspensions are electrically charged [32] due to the amphoteric dissociation of surface Metal-OH groups and adsorption of metal complexes derived from the hydrolysis products of material dissolved from the solid. Titanium in water it is generally covered with hydroxyl groups (A), when the pH is higher than the isoelectric point the surface is negatively charged (B) and the opposite is for pH lower than the pI (C) [33].

$$Ti^{IV} + H_2O \rightarrow Ti^{IV} - OH + H^+ \quad \text{(A)}$$

$$Ti^{IV} - OH + H^+ \rightarrow Ti^{IV} - O^- + H^+ \quad \text{(B)}$$

$$Ti^{IV} - OH + H^+ \rightarrow Ti^{IV} - OH_2^+ \quad \text{(C)}$$

At a pH-value of 4.75 lysine and arginine residues are expected to have a positively net charged by protonation. For the titanium surface a negative charged natural oxide layer is formed that attracts cations at this pH [34]. The main driving force for the compact and rigid layer formation is attributed to the electrostatic interaction with the positive charges of amine and guanidine groups and the formation of hydrogen bonds at pH 4.75 for the Tet-124 and Tet 124-G-DOPA-G.

The peptide adsorption at higher pH (pH = 6.9) was studied; using deionized water as solvent (pH 6.9). The use of buffers such as PBS, Tris (2-Amino-2-hydroxymethylpropane-1,3-diol) or boric buffer was avoided in order to exclude any additional interactions of the buffers with the surface. For example, the phosphate buffer use is known to form complexes with titanium surfaces [35]. Also, pH levels higher than 8 should be avoided because of quinone formation of the catechol moiety due to oxidation. The same peptide concentration was used for the three solutions of different peptide,

however the peptide concentration in water was lower than in acetate buffer by reason of lower solubility in deionized water than in acetate buffer solution.

Figure 4A shows a frequency decrease of −5 Hz for the crystal in contact with the solution of the Tet-124 in water solution, caused by mass adsorption during the first twenty minutes. During the next fifteen minutes no further adsorption of mass was detected. Figure 5A shows the total mass adsorption of 80 ng/cm^2 after saturation. The decrease on mass adsorption of the DOPA-free Tet-124 is attributed to the lower level of protonation of the peptide under more basic conditions.

Figure 4C indicates higher the frequency changes due to mass adsorption of the Tet-124-G-DOPA-G on the titanium surface in comparison with the Tet-124.The small changes in the dissipation coefficient shows a rigid layer, as can be seen in Figure 4B. At an elevated pH value (6.9) the higher adsorption of the DOPA-containing peptide on titanium surfaces is attributed to the enhancement of possible catechol interactions with the titanium surface. The catechol moieties are known to have the properties of charge-transfer complex formation between the catechol groups and Ti^{4+} [35,36]. Catechols can form both covalent and strong non-covalent interactions, such as π-stacking or hydrogen-bond formation. But in general the DOPA adsorption on titanium it is mainly attributed to the formation of mono and bidental complexes [37] of the OH groups. One of the two catechol OH groups dissociates and binds to a metal cation, whereas the second OH group forms an H-bond to the next catechol (monodentate), or alternatively both OH groups dissociate and coordinate with two adjacent metal cations (bidentate) [37]. In general metal coordination complexes [38]

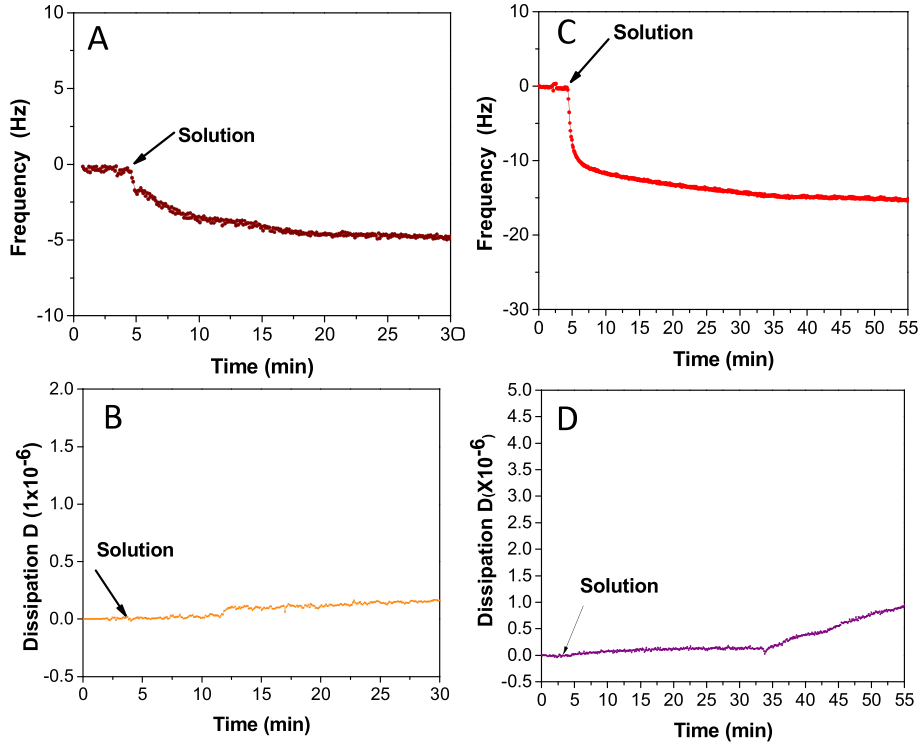

Figure 4 QCM-D measurement A) Frequency B) dissipation. Solution 0.18 mg/ml Tet-124 in deionized water C) Frequency D) dissipation. Solution 0.33 mg/ml Tet-124-G-DOPA-G in deionized water, on titanium coated crystal as function of time.

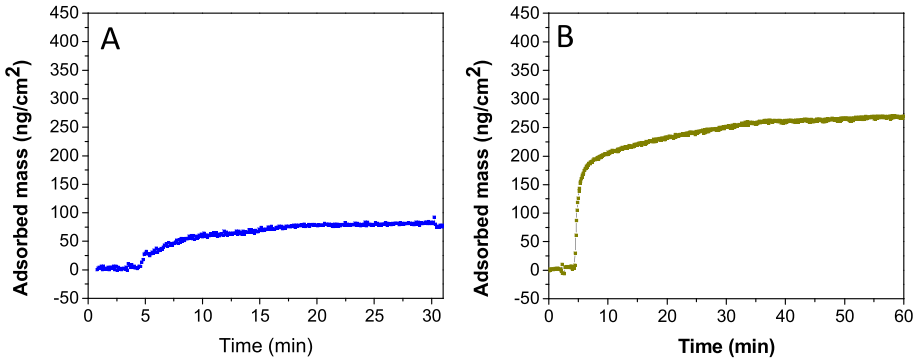

Figure 5 Mass changes obtained from peptide solution on titanium coated sensor, 0.18 mg/ml deionized water A) Tet-124 B) Tet-124-G-DOPA-G.

can be formed where two or more ligands donate a nonbonding electron pair to empty orbitals in a transition metal ion [39]. Several authors explained the formation of metal complexes and the maximum adsorption of catechol containing molecules at pH values higher than 7. The monodentate species dominate at pH up to 5.6, bidentate at a pH from 5.6 to 9.1, and tridentate at pH values higher than 9.1 [38].

Figure 6 shows a scheme of the possible interaction of the peptide Tet-124-G-DOPA-G with the surface.

Figure 7A shows similar adsorption rate behavior between the DOPA-containing peptides G-DOPA-G-Tet-124 and Tet-124-G-DOPA-G. The mass adsorbed in both cases it is approx. 290 ng/cm^2 as shown in Figure 7C. No significant influence of the G-DOPA-G N- and C- terminal modification in the peptide regarding mass adsorption behavior was observed; in both cases a higher adsorption is achieved in

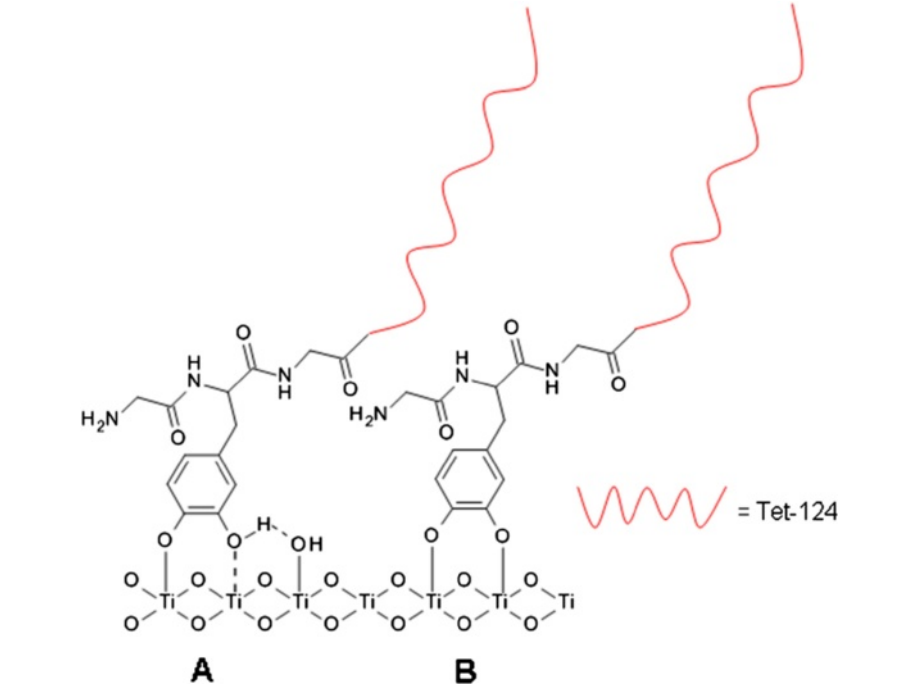

Figure 6 Proposed mechanism of Tet-124-G-DOPA-G binding to titanium surfaces.

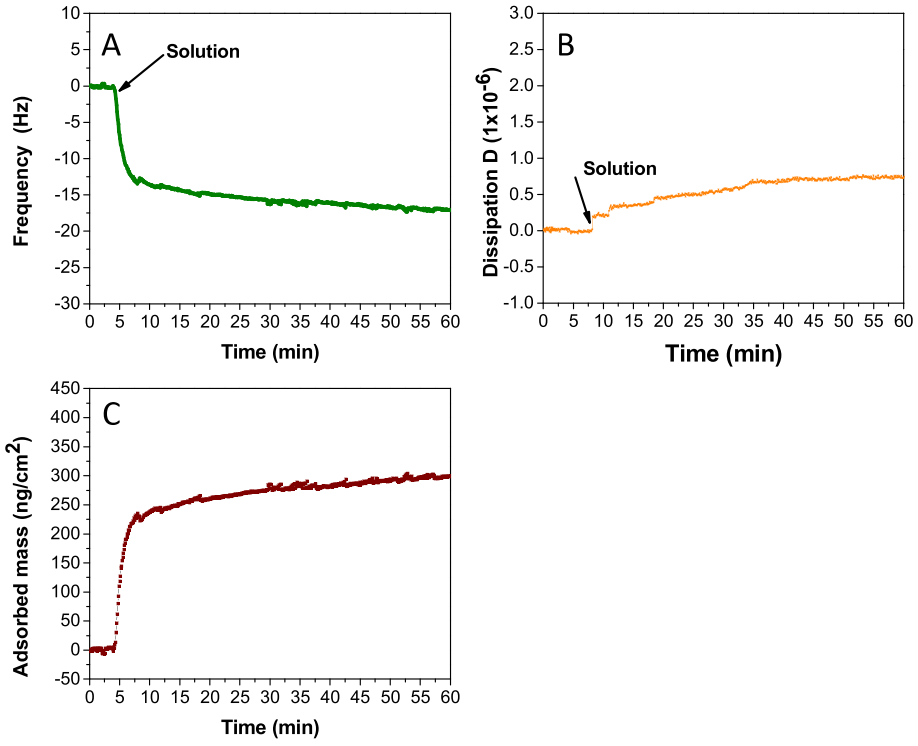

Figure 7 QCM-D measurement of A) Frequency B) dissipation. Solution 0.18 mg/ml G-DOPA-G-Tet-124 in deionized water C) Mass changes. Solution 0.18 mg/ml G-DOPA-G-Tet-124 in deionized water, on titanium coated crystals as function of time.

comparison to the Tet-124 peptide without the G-DOPA-G modification. However the layer formed due to adsorption of the G-DOPA-G-Tet124 presents higher dissipation changes. The driving force for the adsorption of formation of the metal complexes is attributed to the entropic gain associated with the disruption of a highly ordered hydrogen-bonding network of hydrating water molecules; the interplay of electrostatic forces (hard base/hard acid interactions) and complex specific ion/surface interactions [38].

The crystals used in QCM-D were consisted of titanium that differs in composition with the titanium alloy. The titanium coated crystal it is used as a model due to that in both cases it is expected a titanium oxide and titanium abundantly may cover both kinds of the surfaces. Nevertheless the catechol moiety is a hard Lewis base, by its electron donor ability, and that aluminum, titanium and vanadium oxides are hard Lewis acids, thus leading to metal/ligand and coordinative interactions with the metals and metals oxides on the surface of the alloy. In the case of Al_2O_3 a bidentate binding [40], for vanadium (IV) octahedral catechol complex formation [41] and for TiO_2 mostly bidentate complexes are observed in other studies. Also the contact angle of the titanium quartz crystal (same crystals used in this experiment) is approximately 51.25 ± 2.87 accordingly to Neyra, having similar values to the freshly emeried titanium surface that showed (contact angle of 49° ± 5); both surfaces presenting similar hydrophilicity.

It is important to point out that dissimilar coordination environments due to aluminum and vanadium cause different crystalline phase structures and differences in the lattice crystal structure which, consequently alters the surface sites for adsorption

[42]. However a more detailed study of the differences of the sensor and the alloy surface was outside of the scope of this research.

The modification of the titanium alloy surfaces for bacterial and cell adhesion was made with the Tet-124-G-DOPA-G due to the rigid and compact layers formed at different conditions and the possible orientation of the hydrophobic residues to the surface which could interact with the bacteria cell membrane.

The fibroblast cell adhesion was tested in first place to determine if the modification with the peptide could harvest the biocompatibility of the surface. Fibroblasts were left to incubate for 24 h in contact with the titanium alloy sample half modified andthen stained. All the pictures shown below belong to the same half modified sample. Three pictures of each magnification were randomly taken for each sample (50,100 and 200 times referent to 50x, 100x and 200x respectively). The resulting images were a digital merge from the corresponding channels of the fluorescent stains. Image J software was used to add scale bars to the merged pictures, using pictures with known size values as references.

Figure 8 shows the cell behavior after incubation on Ti alloy half modified samples. Figure 6 shows the cell behavior after incubation on Ti samples half modified with the peptide. Cells appear to survive and attach equally well both on the treated and the non-treated surface. In both cases, the cell morphology is typical of well-attached cells under non stressful conditions [43,44], showing many focal adhesion points. The images indicate that biocompatibility and cytotoxicity are similar to that of bare titanium. Titanium is a material widely regarded as biocompatible [45]. The peptide surface modification seems to be biocompatible. The cell density on the surface it is calculated using the Image J for cell counting, at least 3 images from 3 diferent samples were used. The titanium alloy surface shows an average cell density of 5.4×10^4 cell/cm^2 and

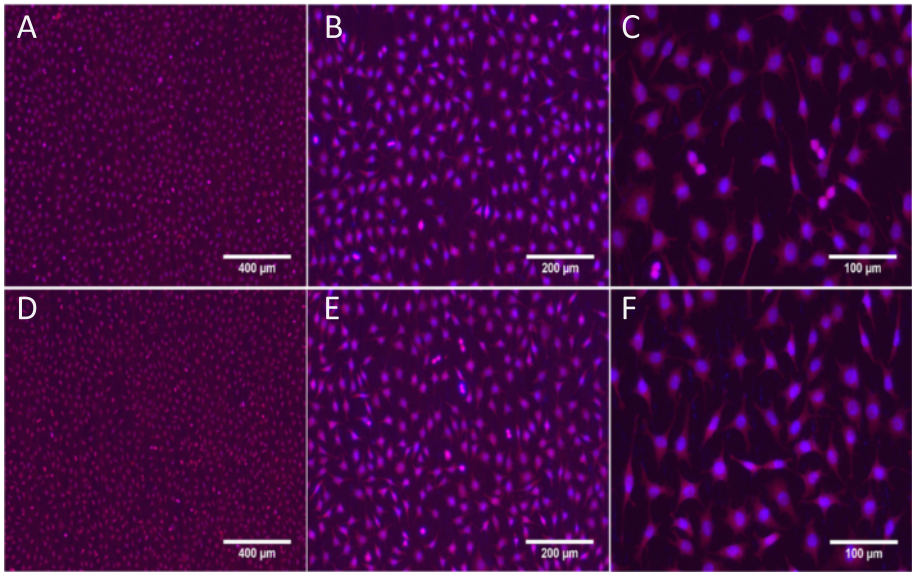

Figure 8 Adhesion test L929 cells incubated 24 h titanium alloy control and titanium modified with the peptide Tet 124- G-DOPA-G A) 50×, control B) 100× control C) 200× control D) 50× modified E) 100× modified F) 200× modified.

the modified sample shows an average a cell density average 4.9×10^4 cell/cm^2, where the difference is within the range of standard deviations.

The aim of a further evaluation was to investigate the antimicrobial activity of the Tet-124-G-DOPA-G peptide against *E. coli* bacteria in aqueous solution and in an immobilized state. The immobilization of the peptide on the titanium surface alters the mobility of the peptide and therefore its interactions with its target [13], making this study of great interest for medical applications. Although titanium alloys such as Ti-6Al-4 V exhibit some antimicrobial activity [46], they are still prone to bacterial colonization, hence the importance of an active compound which can hinder this process and concomitantly favor human cell establishment due to its biocompatibility, which can be accomplished by molecules like antimicrobial peptides. Figure 9 shows the live and dead evaluation of the modified and control Ti-6Al-4 V samples showing that no significant difference in adhesion could be detected after 4 h of contact.

The surface energy properties after the immobilization of Tet-124-G-DOPA-G were studied by contact angle measurements. The contact angle was measured after 24 h in contact with the peptide solution. The freshly emeried titanium surface showed an average contact angle of 49° ± 5. After 24 h in contact with the peptide solution a change from 49° ± 5 to 59° ± 3 was detected; increasing to more hydrophobic values. The surface of the modified sample does not exhibit features such as superhydrophobicity, low roughness or low surface energy, which can give properties of adhesion-repellent to the surface [47]. This could explain the non-relevant change in the attachment behavior. The presence of the peptides (fairly hydrophobic) could, however, lead to a small decrease of adhered cells on the modified samples. On the pictures it is possible to observe that the amount of live and dead cells was similar on both samples (slightly more on the control), suggesting that the presence of the Tet-124-G-DOPA-G did not enhance the quantity of bacteria adhered to the substrate. The green signals (viable bacteria) outnumber the red signals (dead bacteria), which points to a higher amount of viable bacterias. Corroborating the live and dead evaluation Figure 9 shows the results obtained by the bacteria growth from water rinsing after the detachment procedure. The bacteria growth on the control as well as on the peptide modified samples is displayed in the similarity of their *E. coli* growth curves (despite of a slight delay), as shown in Figure 10. Further studies will investigate the antimicrobial properties of the Tet-124-G-DOPA-G immobilized on the surface

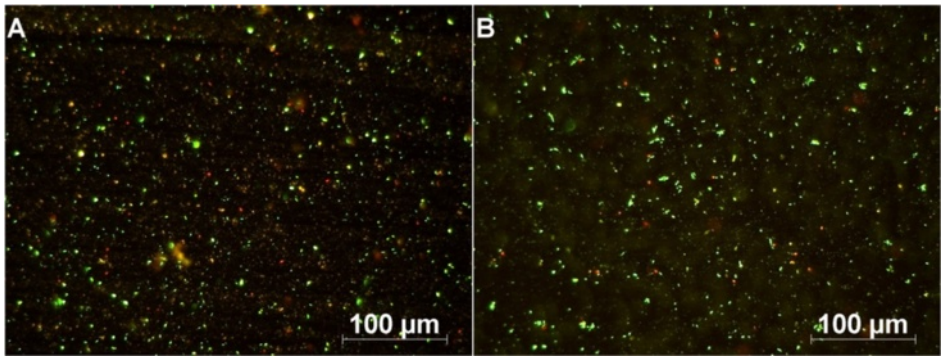

Figure 9 Fluorescence microscopy displaying bacterial viability (green = viable; red = dead) after incubation of 4 hours and stained with LIVE/DEAD® BacLight Bacterial Viability Kit. A) Ti-6Al-4 V control sample **B)** Ti-6Al-4 V sample modified with Tet-124-G-DOPA-G.

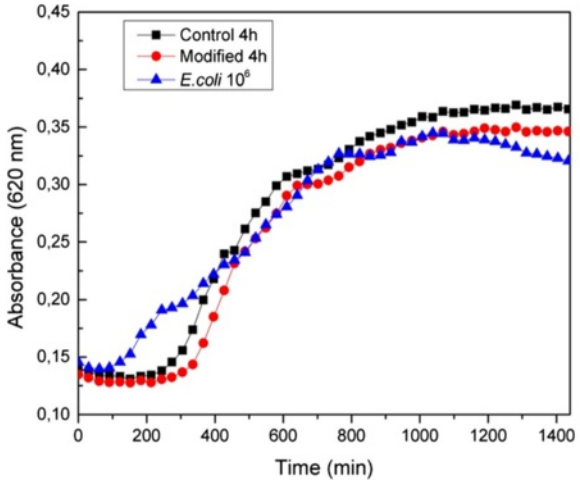

Figure 10 Time-dependent growth of *E.coli* bacteria; solution after detachment procedure; samples 4 hours in surface of titanium alloy control and sample modified Tet-124-G-Dopa-G with growth of *E.coli* suspension of 10^6 CFU/mL.

during longer contact time with the *E. coli* bacteria, along with an analysis using a gram-positive bacteria species and also desorption experiments at different conditions.

Conclusions

The layer formation at pH 4.75 of the Tet-124 and both Tet-124-DOPA specimen is related to the electrostatic interaction with the negatively charged titanium oxide layer. At pH 6.9 the influence of the DOPA moieties enhance the adlayer formation due to the Ti(IV) catechol complexes formation. This study shows that conditions as pH influence on the mass adsorption mass and the stability of the antimicrobial peptide layer on the surface. The modification of the Ti-6Al-44 V with the Tet-124-G-DOPA-G does not change the attachment of *E.coli* bacteria to its surface, however, a longer contact period may be necessary for the peptide to implement its antimicrobial properties. The results indicate also indicate that the surface modification does not influence the biocompatibility and cell attachment of fibroblast to the surface. The G-DOPA-G N and C terminal sequence modification peptide can be used as immobilization strategies of antimicrobial peptides on titanium alloy surfaces.

Competing interests
The authors declare that they have no competing interests.

Author's contributions
All authors drafted the manuscript, read and approved the final manuscript.

Authors' information
Yendry Regina Corrales Urena: Materials Science PhD student, State University of Sao Paulo, UNESP (QCM-D measurements and contact angle).
Matheus Vieira Nascimento: Dentistry undergraduate student; currently performing an internship at Fraunhofer IFAM (Bremen, Germany) with emphasis on microbiological testing of biocompatible materials (In charge of the bacteria adhesion test).
Juliano Luiz Faccioni: Biomedicine undergraduate student; currently performing an internship at Fraunhofer IFAM (Bremen, Germany) with emphasis on cell adhesion and interaction with biomaterials (In charge of the fibroblast cell adhesion test).
Msc. Linda Wittig: Scientific staff Fraunhofer IFAM, adhesives and polymer chemistry department (QCM-D measurements).
Prof. Dr. Paulo Noronha Lisboa Filho: Material Science professor, UNESP State University of Sao Paulo.

Dr. Klaus Rischka: Scientific staff Fraunhofer IFAM, adhesives and polymer chemistry department (Peptide synthesis and Maldi-ToF-MS characterization).

Acknowledgements
The authors thank to Science without Borders (Ciência sem Fronteiras, proc: 88888.015774/2013-00, 88888.020073/2013-00), FAPESP 2013/07296-2 and Consejo Nacional para Investigaciones Científicas y Tecnológicas de Costa Rica (CONICIT) for the funding. Prof. Dr. Bernd Mayer, Prof. Dr. Andreas Hartwig and Dr. Ingo Grunwald for the support and advices.

Author details
[1]Programa de Pós-Graduação em Ciência e Tecnologia de Materiais (POSMAT), São Paulo State University (UNESP), Av. Eng. Luiz Edmundo Carrijo Coube 14-01, 17033-360, Bauru, São Paulo, Brazil. [2]Fraunhofer Institute for Manufacturing Technology and Advanced Materials (IFAM), Wiener Straße 12, 28359 Bremen, Germany. [3]Federal University of Ceará, Av. Da Universidade 2853, 60020-181 Fortaleza, Ceará, Brazil. [4]Federal University of Rio Grande do Sul, Rua Sarmento Leite 500, 90040-060 Porto Alegre, RS, Brazil. [5]São Paulo State University (UNESP), Av. Eng. Luiz Edmundo Carrijo Coube 14-01, 17033-360 Bauru, São Paulo, Brazil.

Received: 21 November 2014 Accepted: 30 January 2015
Published online: 15 March 2015

References

1. Zhao L, Hu Y, Xu D, Cai K (2014) Surface functionalization of titanium substrates with chitosan–lauric acid conjugate to enhance osteoblasts functions and inhibit bacteria adhesion. Colloids Surf B Biointerfaces 119:115–125. doi:10.1016/j.colsurfb.2014.05.002
2. Das K, Bose S, Bandyopadhyay A, Karandikar B, Gibbins BL (2008) Surface coatings for improvement of bone cell materials and antimicrobial activities of Ti implants. J Biomed Mater Res 87B:455–460. doi:10.1002/jbm.b.31125
3. Al-Radha ASD, Dymock D, Younes C, O'Sullivan D (2012) Surface properties of titanium and zirconia dental implant materials and their effect on bacterial adhesion. J Dent 40:146–153. doi:10.1016/j.jdent.2011.12.006
4. Park S, Park Y, Hahm K-S (2011) The role of antimicrobial peptides in preventing multidrug-resistant bacterial infections and biofilm formation. IJ Mol Sci 12:5971–5992. doi:10.3390/ijms12095971
5. Kazemzadeh-Narbat M, Kindrachuk J, Duan K, Jenssen H, Hancock RE, Wang R (2010) Antimicrobial peptides on calcium phosphate-coated titanium for the prevention of implant-associated infections. Biomaterials 31:9519–9526. doi:10.1016/j.biomaterials.2010.08.035
6. Svensson S, Suska F, Emanuelsson L, Palmquist A, Norlindh B, Trobos M, Bäckros H, Persson L, Rydja G, Ohrlander M, Lyvén B, Lausmaa J, Thomsen P (2013) Osseointegration of titanium with an antimicrobial nanostructured noble metal coating. Nanomed Nanotech Biol Med 9:1048–1056. doi:10.1016/j.nano.2013.04.009
7. Massa MA, Covarrubias C, Bittner M, Fuentevilla IA, Capetillo P, von Marttens A, Carvajal JC (2014) Synthesis of new antibacterial composite coating for titanium based on highly ordered nanoporous silica and silver nanoparticles. Mater Sci Eng C 45:146–153. doi:10.1016/j.msec.2014.08.057
8. Murakami A, Arimoto T, Suzuki D, Iwai-Yoshida M, Otsuka F, Shibata Y, Igarashi T, Kamijo R, Miyazaki T (2012) Antimicrobial and osteogenic properties of a hydrophilic-modified nanoscale hydroxyapatite coating on titanium. Nanomed Nanotech Biol Med 8:374–382. doi:10.1016/j.nano.2011.07.001
9. Lv H, Chen Z, Yang X, Cen L, Zhang X, Gao P (2014) Layer-by-layer self-assembly of minocycline-loaded chitosan/alginate multilayer on titanium substrates to inhibit biofilm formation. J Dent 42:1464–1472. doi:10.1016/j.jdent.2014.06.003
10. Yoshinari M, Kato T, Matsuzaka K, Hayakawa T, Shiba K (2010) Prevention of biofilm formation on titanium surfaces modified with conjugated molecules comprised of antimicrobial and titanium-binding peptides. Biofouling 26:103–110. doi:10.1080/08927010903216572
11. de la Fuente-Nunez C, Korolik V, Bains M, Nguyen U, Breidenstein EBM, Horsman S, Lewenza S, Burrows L, Hancock REW (2012) Inhibition of bacterial biofilm formation and swarming motility by a small synthetic cationic peptide. Antimicrob Agents Chemother 56:2696–2704. doi:10.1128/AAC. 00064-12
12. Easton DM, Nijnik A, Mayer ML, Hancock RE (2009) Potential of immunomodulatory host defense peptides as novel anti-infectives. Trends Biotech 27:582–590. doi:10.1016/j.tibtech.2009.07.004
13. Hilpert K, Elliott M, Jenssen H, Kindrachuk J, Fjell CD, Körner J, Winkler DF, Weaver LL, Henklein P, Ulrich AS (2009) Screening and characterization of surface-tethered cationic peptides for antimicrobial activity. Chem Biol 16:58–69. doi:10.1016/j.chembiol.2008.11.006
14. Hancock REW, Sahl H-G (2006) Antimicrobial and host-defense peptides as new anti-infective therapeutic strategies. Nat Biotechnol 24:1551–1557. doi:10.1038/nbt1267
15. Hilpert K, Elliott MR, Volkmer-Engert R, Henklein P, Donini O, Zhou Q, Winkler DF, Hancock RE (2006) Sequence requirements and an optimization strategy for short antimicrobial peptides. Chem Biol 13:1101–1107. doi:10.1016/j.chembiol.2006.08.014
16. Lee H, Rho J, Messersmith PB (2009) Facile conjugation of biomolecules onto surfaces via mussel adhesive protein inspired coatings. Adv Mater 21:431–434. doi:10.1002/adma.200801222
17. Haynie SL, Crum GA, Doele BA (1995) Antimicrobial activities of amphiphilic peptides covalently bonded to a water-insoluble resin. Antimicrob Agents Chemother 39(2):301–307
18. Von Byern J, Grunwald I (2010) Biological adhesion systems: From nature to technical and medical application. Springer, Wien, New York, London
19. Rischka K, Müller FA, Diaconu G, Amkreutz M, Richter K, Hartwig A (2013) Adsorption studies of mussel-inspired peptides. Bioinsp, Biomimet and Nanobiomat 2:45–53. doi:10.1680/bbn.12.00022
20. Neyra, MP. Interactions between titanium surfaces and biological components. Universitat Politècnica de Catalunya. PhD Thesis dissertation.

21. Dixon MC (2008) Quartz crystal microbalance with dissipation monitoring: Enabling real-time characterization of biological materials and their interactions. J Biomol Tech 19:151–158
22. Jordan JL, Fernandez EJ (2008) QCM-D sensitivity to protein adsorption reversibility. Biotechnol Bioeng 101:837–842. doi:10.1002/bit.21977
23. Q-Sense. Quartz crystal microbalance with dissipation (QCM-D). Technology Note.
24. Life Technologies. Actin staining protocol. https://www.lifetechnologies.com/de/de/home/references/protocols/cell-and-tissue-analysis/microscopy-protocol/actin-staining-protocol.html.html. Accessed on 20 November 2014.
25. Hovgaard MB, Dong M, Otzen DE, Besenbacher F (2007) Quartz crystal microbalance studies of multilayer glucagon fibrillation at the solid–liquid interface. Biophys J 93:2162–2169. doi:10.1529/biophysj.107.109686
26. Deligöz H, Tieke B (2014) QCM-D study of layer-by-layer assembly of polyelectrolyte blend films and their drug loading-release behavior. Colloid Surface A 441:725–736. doi:10.1016/j.colsurfa.2013.10.033
27. Q-Sense. Study of viscoelastic films – a comparison between the Voigt viscoelastic model and the Sauerbrey relation. Application Note QS 405-07-2. www.q-sense.com
28. Sebők D, Csapó E, Preočanin T, Bohus G, Kallay N, Dékány I (2013) Adsorption of ibuprofen and dopamine on functionalized gold using Surface plasmon resonance spectroscopy at solid–liquid interface. Croat Chem Acta 86:287–295. doi:10.5562/cca2343
29. Protein Calculator v3.4. 2013. http://protcalc.sourceforge.net/. Accessed on 20 November 2014.
30. Rabe M, Verdes D, Seeger S (2011) Understanding protein adsorption phenomena at solid surfaces. Adv Colloid Interface Sci 162:87–106. doi:10.1016/j.cis.2010.12.007
31. Cuddy FM, Poda AR, Brantley LN (2013) Determination of isoelectric points and the role of pH for common quartz crystal microbalance sensors. ACS Appl Mater Interfaces 5:3514–3518. doi:10.1021/am400909g
32. Parks GA (1965) The isoelectric points of solid oxides, solid hydroxides, and aqueous hydroxo complex systems. Chem Rev 65(2):177–198
33. Suttiponparnit K, Jiang J, Sahu M, Suvachittanont S, Charinpanitkul T, Biswas P (2010) Role of surface area, primary particle size, and crystal phase on titanium dioxide nanoparticle dispersion properties. Nanoscale Res Lett 39:20460. doi:10.1007/s11671-010-9772-1
34. Kabaso D, Gongadze E, Perutková Š, Matschegewski C, Kralj-Iglič V, Beck U, van Rienen U, Iglič A (2011) Mechanics and electrostatics of the interactions between osteoblasts and titanium surface. Comput Method in Biomech 14:469–482. doi:10.1080/10255842.2010.534986
35. Wei Q, Becherer T, Mutihac R-C, Noeske P-LM, Paulus F, Haag R, Grunwald I (2014) Multivalent anchoring and cross-linking of mussel-inspired antifouling surface coatings. Biomacromolecules 15:3061–3071. doi:10.1021/bm500673u
36. Araujo PZ, Morando PJ, Blesa MA (2005) Interaction of catechol and gallic acid with titanium dioxide in aqueous suspensions. 1. Equilibrium Studies. Langmuir 21:3470–3474. doi:10.1021/la0476985
37. Ye Q, Zhou F, Liu W (2011) Bioinspired catecholic chemistry for surface modification. Chem Soc Rev 40:4244–4258. doi:10.1039/c1cs15026j
38. Petrone L (2013) Molecular surface chemistry in marine bioadhesion. Adv Colloid Interface Sci 195–196:1–18. doi:10.1016/j.cis.2013.03.006
39. Xu Z (2013) Mechanics of metal-catecholate complexes: the roles of coordination state and metal types. Sci Rep 3:2914. doi:10.1038/srep02914
40. Connor PA, Dobson KD, McQuillan AJ (1995) New sol–gel attenuated total reflection infrared spectroscopic method for analysis of adsorption at metal oxide surfaces in aqueous solutions. Chelation of TiO_2, ZrO_2, and Al_20_3 Surfaces by catechol, 8-quinolinol, and acetylacetone. Langmuir 11:4193–4195
41. Borgias BA, Cooper SR, Koh YB, Raymond KN (1984) Synthetic, structural, and physical studies of titanium complexes of catechol and 3,5-Di-tert-butylcatechol. Inorg Chem 23:1009–1016
42. Rodriguez R, Blesa MA, Regazzoni AE (1996) Surface complexation at the TiO2 (anatase)/aqueous solution interface: Chemisorption of catechol. J Colloid Interface Sci 177:122–131
43. Ponsonnet L, Comte V, Othmane A, Lagneau C, Charbonnier M, Lissac M, Jaffrezic N (2002) Effect of surface topography and chemistry on adhesion, orientation and growth of fibroblasts on nickel–titanium substrates. Mater Sci Eng C 21:157–165. doi:10.1016/S0928-4931(02)00097-8
44. Linez-Bataillon P, Monchau F, Bigerelle M, Hildebrand H (2002) In vitro MC3T3 osteoblast adhesion with respect to surface roughness of Ti6Al4V substrates. Biomol Eng 19:133–141. doi:10.1016/S1389-0344(02)00024-2
45. Eisenbarth E, Velten D, Schenk-Meuser K, Linez P, Biehl V, Duschner H, Breme J, Hildebrand H (2002) Interactions between cells and titanium surfaces. Biomol Eng 19:243–249. doi:10.1016/S1389-0344(02)00032-1
46. Walkowiak-Przybyło M, Klimek L, Okrój W, Jakubowski W, Chwiłka M, Czajka A, Walkowiak B (2012) Adhesion, activation, and aggregation of blood platelets and biofilm formation on the surfaces of titanium alloys Ti6Al4V and Ti6Al7Nb. J Biomed Mater Res 100A:768–775. doi:10.1002/jbm.a.34006
47. Campoccia D, Montanaro L, Arciola CR (2013) A review of the biomaterials technologies for infection-resistant surfaces. Biomaterials 34:8533–8554. doi:10.1016/j.biomaterials.2013.07.089